Evolution of collectivity and shape transition in ^{66}Zn

S. Rai,[1,*] U. S. Ghosh,[1] B. Mukherjee,[1,†] A. Biswas,[1] A. K. Mondal,[1] K. Mandal,[1] A. Chakraborty,[1] S. Chakraborty,[2,‡] G. Mukherjee,[3] A. Sharma,[4] I. Bala,[5] S. Muralithar,[5] and R. P. Singh[5]

[1]*Department of Physics, Siksha-Bhavana, Visva-Bharati, Santiniketan, West Bengal-731235, India*
[2]*Department of Physics, Institute of Science, Banaras Hindu University, Varanasi-221005, India*
[3]*Variable Energy Cyclotron Centre (VECC), 1/AF Bidhannagar, Kolkata-700064, India*
[4]*Department of Physics, Himachal Pradesh University, Shimla-171005, India*
[5]*Inter University Accelerator Centre (IUAC), Aruna Asaf Ali Marg, New Delhi-110067, India*

(Received 22 August 2020; accepted 16 November 2020; published 14 December 2020)

Excited states in ^{66}Zn were investigated through the in-beam γ-ray spectroscopic techniques using the ^{52}Cr(^{18}O, $2p2n$) fusion-evaporation reaction at a beam energy of 72.5 MeV. The γ-rays emitted by the de-exciting nuclei were recorded in coincidence mode using the 14 Compton suppressed Ge clover detectors of the Indian National Gamma Array. With 14 new transitions being identified, the level scheme of ^{66}Zn has been extended up to the excitation energy $\approx$12.3 MeV and spin $\approx$17 $\hbar$. A rotational band, associated with the two quasineutrons from the $1g_{9/2}$ orbital, has been found to exhibit a band crossing with the ground-state band at a spin of 6$\hbar$. The evolution of the collectivity and shape transition in this nucleus have been discussed in the framework of the total Routhian surface calculations and in comparison with the neighboring ^{68,70}Ge nuclei.

DOI: 10.1103/PhysRevC.102.064313

I. INTRODUCTION

Nuclei in the mass region $A \approx 60$–70 having its Fermi surfaces lying in between that of the $N = Z = 28$ doubly magic ^{56}Ni and the semi-magic $N = 40$ subshell gap are known to exhibit a complex interplay of the single-particle and the collective modes of excitation. While the single particle excitation involves the valence nucleons outside the ^{56}Ni core, the collective excitation has been attributed to the gaps observed in the Nilsson energy diagram at $N = Z = 34$, 36 for the oblate deformation and $N = Z = 38$ for the prolate deformation. In this mass region, the high-j unique parity $1g_{9/2}$ orbital is found to play a major role in the configuration of high spin states and it has been attributed in producing several exciting high spin phenomena [1–8]. Collective structures arising out of the different quasiparticle configurations based on the $\pi 1g_{9/2}$ and/or $\nu 1g_{9/2}$ orbitals have been found to give rise to the different kinds of shape evolution with the increasing spin. In this mass region, the octupole correlations are also expected due to the presence of orbitals satisfying $\Delta L = \Delta J = 3$ criterion, arising out of the $2p_{3/2}$ ($L = 1$) and the $1g_{9/2}(L = 4)$ orbitals around the Fermi surface.

Lying in the transitional region encompassing the doubly magic spherical ^{56}Ni and the strongly deformed Sr, Kr isotopes, ^{66}Zn is an interesting candidate for studying the phenomena of shape transitions from the spectroscopic point of view. In the neighboring nuclei, the alignment of the neutrons and protons in the $1g_{9/2}$ orbitals have been observed leading to the band crossing between the collective structures of different configurations [9–14]. Several superdeformed and terminating bands have been reported in the lighter Zn and other slightly heavier even-even ^{68,70}Ge isotopes [3,4,9–12]. These observations have motivated us for studying the nuclear structure in ^{66}Zn, the latest studies of which date back to the 1970s. Furthermore, most of the previously reported level-structure investigations were performed using the β-decays [15,16], transfer reactions [17] or light-ion induced reactions [18–22] with modest experimental setups. Moreover, Morand *et al.* [23] have measured the lifetimes of a few yrast states in ^{66}Zn via the Doppler shift attenuation method (DSAM), while Cleemann *et al.* [21] have measured lifetimes of some of the negative parity levels using the recoil Doppler method (RDM).

In this article, we report for the first time on the high spin states in ^{66}Zn populated using a heavy-ion induced reaction. The emitted γ-rays were detected with a high resolution and efficient array of high-purity germanium (HPGe) clover detectors. The level scheme of ^{66}Zn has been revisited using the γ-γ coincidence technique and extended significantly in the present work. A collective band based on two $1g_{9/2}$ quasineutrons has been found to exhibit a band crossing with the ground-state band at a spin of 6$\hbar$. The evolution of the collectivity and shape transition in this nucleus have been discussed in the framework of the total Routhian surface (TRS) calculation and compared with the neighboring ^{68,70}Ge nuclei, which have similar kind of collective features.

II. EXPERIMENTAL DETAILS AND DATA ANALYSIS

The fusion evaporation reaction ^{52}Cr(^{18}O, $2p2n$) at a beam energy of $E_{lab} = 72.5$ MeV was used to populate the high

*Present address: Forensic Science Laboratory, 37/1/2 Belgachia Road, Kolkata-700037, India.
†buddhadev.mukherjee@visva-bharati.ac.in
‡Present address: Inter University Accelerator Centre, New Delhi.

spin states in ^{66}Zn. The ^{18}O beam was delivered by the tandem accelerator of Inter University Accelerator Center (IUAC), New Delhi [24]. The isotopic ^{52}Cr target of thickness ≈1.0 mg cm^{-2} was prepared by evaporation on a ^{197}Au backing of thickness ≈8 mg cm^{-2}. The γ-rays emitted by the de-exciting nuclei were recorded in coincidence mode (two- or higher-fold of γ transitions) by the 14 Compton suppressed HPGe Clover detectors of the Indian National Gamma Array (INGA) [25] at IUAC. A total of about 2×10^9 events, in which at least two clover detectors have fired in coincidence, were collected in a list-mode format using the CANDLE [26] data acquisition software. Further analysis of the coincidence data were performed using the INGAsort [27] and the RADWARE [28] suites of program. The multipolarity of the observed transitions were determined from an angular correlation analysis using the method of directional correlation from oriented states (DCO) [29]. To determine the electric or the magnetic nature of the γ-ray transitions from the coincidence data, the polarization asymmetry of the Compton scattered photons was measured [30,31]. More details of the experimental set up and the procedure of data analysis can be found in Refs. [32–34].

III. RESULTS AND LEVEL SCHEME

Based on the known ground-state spin-parity, γ-γ coincidence arguments, intensities of γ-rays, angular correlation and the polarization analysis, we have proposed a new level scheme of ^{66}Zn, which is shown in the Fig. 1. The new transitions found in this work are marked with the asterisks (*) and the tentative spin-parity assignments are given in the parentheses. Table I summarizes the experimental information on the level structure of ^{66}Zn, obtained in this work. The level scheme has been extended up to an excitation energy of ≈12.3 MeV and spin ≈ $(17^+)\hbar$. Fourteen new γ-ray transitions have been identified and placed in the level scheme of ^{66}Zn, apart from confirming the tentatively assigned spin-parity of the established levels reported in the previous studies [19–21].

The previously established [19–21] 4^+, 6^+, and 8^+ levels of the ground-state band at the 2450, 4179, and 5205 keV, respectively, have been confirmed in this work following the coincidence relationship, intensity arguments, R_{DCO} and the polarization asymmetry values of the 1411, 1729, and 1026 keV γ-ray transitions. Above the 8^+ level, two levels have been reported to decay by a cascade of 1086 and 1226 keV γ-ray transitions, spin-parity of which were assigned tentatively in the previous investigation [20]. The angular correlation and polarization measurements of these transitions confirm the tentatively assigned spin-parity of the 10^+ to the 6291 keV level and 12^+ to the 7517 keV level. Above the 12^+ state, several new levels have been identified and placed in the level scheme on the basis of γ-γ coincidence analysis. A new state has been identified at 9304 keV which decays by a 1787 keV γ-ray transition to the 12^+ level. The multipolarity of this transition has been found to be quadrupole in nature, evident from the DCO ratio with the gates on the quadrupole transitions of ^{66}Zn. This state is also found to decay to the 10^+ level via an intermediate (12^+) level at 7918 keV by a cascade

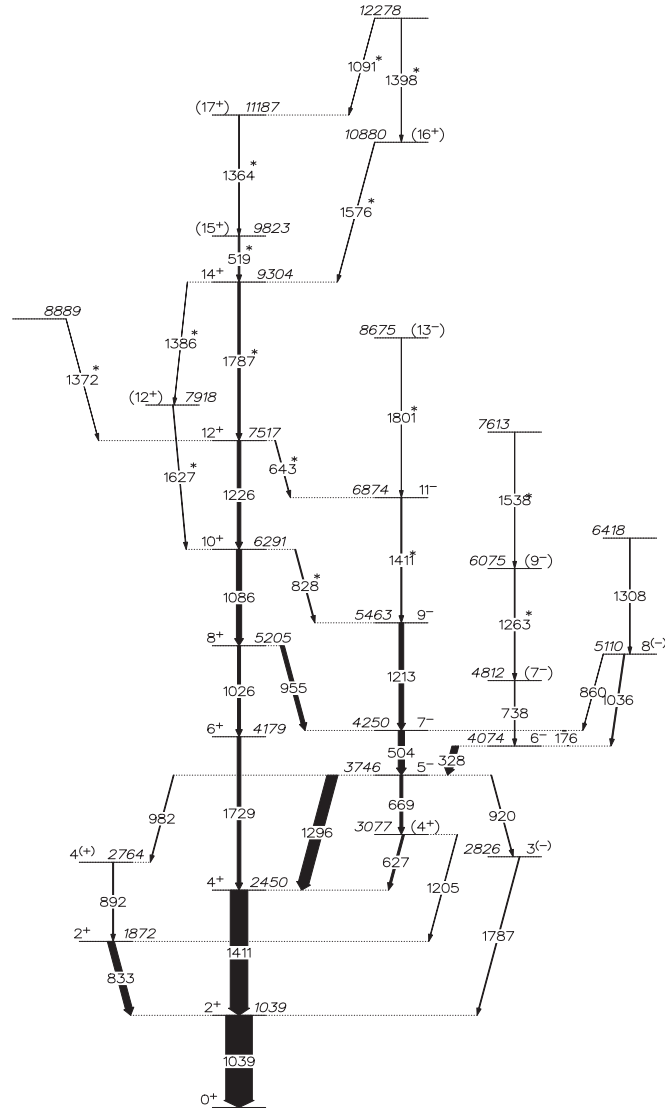

FIG. 1. Proposed level scheme for ^{66}Zn as deduced from the present investigation. All the transitions have been placed based on the γ-γ coincidence relationships and the width of the arrows corresponds to the relative γ-ray intensity. The level energies and the γ-ray energies are given in the units of keV. The newly identified transitions are marked with the asterisks(*) and the tentatively assigned spin-parities are given in parentheses. See text and Table I for more details.

of the 1386 and 1627 keV γ-ray transitions. Above the 9304 keV level, a new state has been identified at 9823 keV, which decays to the 9304 keV level by a 519 keV transition. Though the polarization asymmetry value could not be determined for this transition, considering its R_{DCO} and the intensity value, the 9823 keV state is assigned with a spin-parity of (15^+). The level at 9304 keV is fed by a cascade of the 1576 and 1398 keV γ-ray transitions. A tentative value of spin-parity (16^+) has been assigned for the 10 880 keV level, whereas no assignment could be made for the 12 278 keV level. The latter level decays to the 9823 keV state via a cascade of the 1091 and 1364 keV γ-ray transitions. Three background subtracted

TABLE I. Values of the level energies (E_i) in keV, γ-ray energies (E_γ) in keV, initial (I_i^π) → final (I_f^π) spin-parity, relative intensities (I_γ), DCO ratio (R_{DCO}), and polarization asymmetry (Δ_{asym}) of the γ-ray transitions as obtained in this work for ^{66}Zn.

Level energy E_i(keV)	Gamma-ray energy E_γ(keV)	Initial → Final spin-parity $I_i^\pi \rightarrow I_f^\pi$	Relative Intensity[a] I_γ	DCO ratio R_{DCO}	Polarization asymmetry Δ_{asym}	Assignment
1039	1038.91(13)	$2^+ \rightarrow 0^+$	100(3)	1.01(9)[c]	0.14(4)	$E2$
1872	833.19(19)	$2^+ \rightarrow 2^+$	25.72(92)	0.88(8)[b]	−0.16(6)	$M1(+E2)$
2450	1411.14(15)	$4^+ \rightarrow 2^+$	$62 < I_\gamma < 69$	1.03(13)[f]	0.12(4)	$E2$
2764	891.91(19)	$4^{(+)} \rightarrow 2^+$	3.77(26)	1.32(27)[b]		$(E2)$
2826	1787.32(13)[d]	$3^{(-)} \rightarrow 2^+$	<3			
3077	627.20(18)	$(4^+) \rightarrow 4^+$	8.00(38)	0.86(26)[b]		$(M1)$
	1205.21(14)	$(4^+) \rightarrow 2^+$	2.13(21)	1.01(20)[b]		$(E2)$
3746	668.80(21)	$5^- \rightarrow (4^+)$	10.96(47)	0.77(13)[b]		$(E1)$
	920.34(17)	$5^- \rightarrow 3^{(-)}$	2.81(23)	1.28(30)[b]		$(E2)$
	981.72(15)	$5^- \rightarrow 4^{(+)}$	2.80(23)	0.46(20)[b]		$(E1)$
	1296.34(11)	$5^- \rightarrow 4^+$	40.15(140)	0.57(4)[b]	0.12(7)	$E1$
4074	328.40(17)	$6^- \rightarrow 5^-$	24.80(89)	0.70(5)[b]	0.11(9)	$M1+E2$
4179	1728.67(18)	$6^+ \rightarrow 4^+$	13.57(55)	1.09(13)[b]	0.13(8)	$E2$
4250	176.34(14)	$7^- \rightarrow 6^-$	11.97(50)	0.76(6)[b]		$M1+E2$
	504.45(15)	$7^- \rightarrow 5^-$	23.38(85)	1.05(9)[b]	0.08(5)	$E2$
4812	738.45(15)	$(7^-) \rightarrow 6^-$	2.33(21)	0.83(27)[b]		$(M1+E2)$
5110	860.13(18)[e]	$8^{(-)} \rightarrow 7^-$	1.30(18)			
	1035.90(17)	$8^{(-)} \rightarrow 6^-$	4.20(27)	1.09(22)[b]		$(E2)$
5205	1026.46(18)	$8^+ \rightarrow 6^+$	11.25(48)	1.06(14)[b]	0.04(2)	$E2$
	954.42(21)	$8^+ \rightarrow 7^-$	15.23(60)	0.47(5)[b]		$E1$
5463	1213.22(14)	$9^- \rightarrow 7^-$	17.63(67)	1.13(13)[b]	0.08(1)	$E2$
6075	1262.89(15)	$(9^-) \rightarrow (7^-)$	2.83(14)	1.20(27)[b]		$(E2)$
6291	1085.65(10)	$10^+ \rightarrow 8^+$	19.75(74)	1.00(10)[b]	0.06(4)	$E2$
	827.80(13)	$10^+ \rightarrow 9^-$	3.70(26)	0.45(10)[c]		$E1$
6418	1308.15(23)	$\rightarrow 8^{(-)}$	1.03(18)			
6874	1411.11(13)	$11^- \rightarrow 9^-$	<4	1.10(18)[c]	0.05(1)	$E2$
7517	1225.56(16)	$12^+ \rightarrow 10^+$	13.39(55)	1.06(16)[b]		$E2$
	642.77(16)	$12^+ \rightarrow 11^-$	2.64(22)			
7613	1537.97(19)	$\rightarrow (9^-)$	0.65(11)			
7918	1627.30(24)	$(12^+) \rightarrow 10^+$	2.08(10)	0.78(20)[f]		$(E2)$
8675	1800.63(31)[e]	$(13^-) \rightarrow 11^-$	<1			
8889	1371.75(22)[e]	$\rightarrow 12^+$	<1			
9304	1787.13(19)	$14^+ \rightarrow 12^+$	<10	1.15(28)[c]		$(E2)$
	1385.58(18)	$14^+ \rightarrow (12^+)$	0.77(17)			
9823	518.74(19)	$(15^+) \rightarrow 14^+$	5.90(32)	0.64(16)[b]		$M1+E2$
10880	1575.62(30)	$(16^+) \rightarrow 14^+$	1.60(19)	0.83(14)[c]		$(E2)$
11187	1364.41(21)	$(17^+) \rightarrow (15^+)$	0.72(17)	1.05(66)[f]		$(E2)$
12278	1090.65(18)[e]	$\rightarrow (17^+)$	<1			
	1398.41(24)[e]	$\rightarrow (16^+)$	<1			

[a]The quoted error includes the fitting error plus an additional error of 3% taken due to the uncertainties in efficiency, background subtraction, etc.
[b]Gate on $E2$, 1039 keV.
[c]Gate on $E2$, 1411 keV.
[d]Measurement of R_{DCO} and Intensity were not possible due to the presence of overlapping γ-energies.
[e]Measurement of R_{DCO} or Intensity were not possible due to the weak statistics.
[f]Gate on $E2$, 1086 keV.

γ-γ coincidence spectra gated by the 1039, 1411 and 519 keV transitions of ^{66}Zn are shown, respectively, in Figs. 2(a)–2(c), wherein most of the new transitions reported in the present work can be seen.

Apart from the ground-state band structure, the positive parity structures have also been established [19–21], which are weakly populated in the present work. The 1872 keV level decaying to the yrast 2^+ level by the 833 keV γ-ray transition, has been observed in conformity with the earlier spin-parity assignment 2^+. This state is fed by a 1205 keV transition and a relatively intense 892 keV transition, both having the quadrupole nature as evident from their DCO ratios. The (4^+) level at 3077 keV is fed by a 669 keV transition of $E1$ nature from the strongly populated 5^- state at 3746 keV. It decays

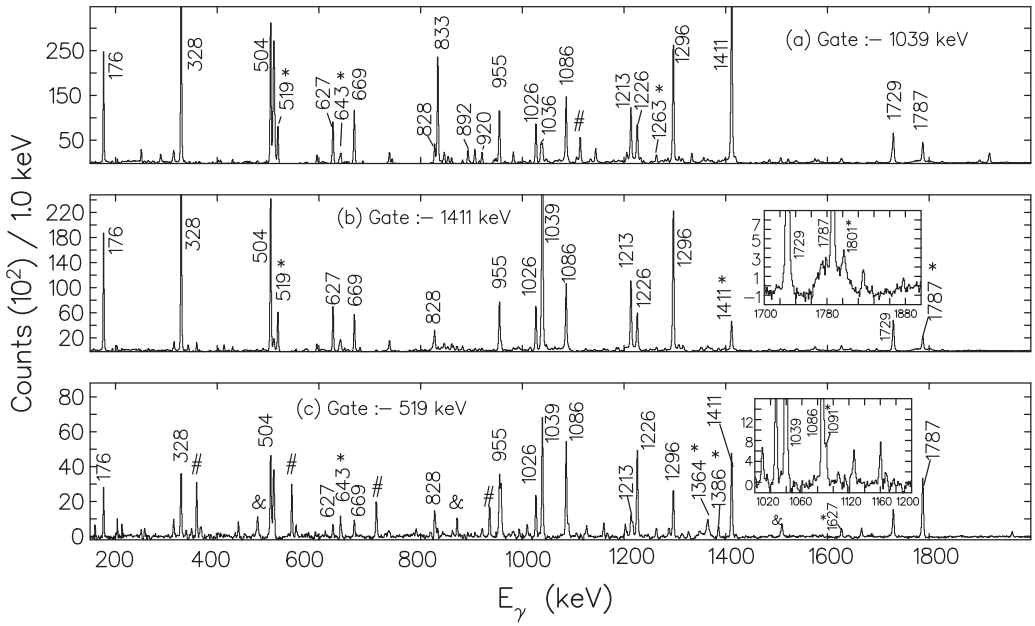

FIG. 2. Background subtracted γ-γ coincidence spectra for ^{66}Zn gated on (a) 1039 keV ($2^+ \rightarrow 0^+$), (b) 1411 keV ($4^+ \rightarrow 2^+$), which also contains the contribution from the 1411 keV($11^- \rightarrow 9^-$) transition. The inset shows the newly identified 1801 keV transition along with the 1729 keV and the 1787 keV transitions, and (c) 519 keV ($(15^+) \rightarrow 14^+$) transition. The inset shows the newly identified 1091 keV transition along with the 1089 keV transition. Here, y-axis represents counts per 1.0 keV. New transitions are marked by the asterisks (*). Strong peaks which are marked with the "#" indicate contaminant γ-rays and those marked by the "&" represent transitions which may belong to ^{66}Zn but could not be placed in the level scheme due to the insufficient coincidence statistics. Here, the contaminant γ-rays are appearing from the ^{61,62}Cu and ^{67}Ga nuclei which are also populated in the same fusion evaporation reaction.

via the 627 keV γ-ray transition to the yrast 4^+ level at the 2450 keV and to the 1872 keV level via the 1205 keV γ-ray transition.

The lowest negative parity state at 2826 keV which was previously established as the 3^- from angular correlation of the de-exciting 1787 keV transition [19], is weakly populated in the present reaction. Due to the presence of an overlapping 1787 keV transition, a firm spin-parity assignment to this state could not be done. This state is fed by a weak 920 keV transition from the 3746 keV level. The 3746 keV level is strongly populated which decays dominantly to the 4_1^+ state. The R_{DCO} and the polarization asymmetry values of the 1296 keV transition feeding the 2450 keV level confirm the 5^- spin-parity assignment to 3746 keV state. Above this level, three strongly populated negative parity states, viz, the 6^- at 4074 keV, 7^- at 4250 keV and the 9^- at 5463 keV, which have been previously established, are confirmed as evident from the electromagnetic nature of the 328, 504, and the 1213 keV transitions, respectively. This sequence is extended by two new levels, one at 6874 keV with the spin-parity 11^- and the other at 8675 keV for which no spin-parity could be assigned due to its weak intensity. The three members of the negative parity sequence i.e, the 7^-, 9^-, and 11^- states are found to be connected to the yrast positive parity states, namely 8^+, 10^+, and 12^+, respectively, by the 955, 828, and 643 keV transitions. A negative parity sequence built on the 6^-, 4074 keV state has been extended with the addition of two new levels at 6075 and 7613 keV. Another cascade of the 1036 and 1308 keV transitions feeding the 6^- level is observed in accordance with the previous work [20], however spin-parity assignment could not be done for the 6418 keV state due to the weak intensity of the transition decaying from the state. A background subtracted γ-γ coincidence spectrum gated by the newly identified 519 keV transition of ^{66}Zn is shown in Fig. 2(c), wherein most of the transitions reported in the present work can be observed.

IV. DISCUSSION

^{66}Zn has two protons and eight neutrons outside the doubly magic core, ^{56}Ni. In the valence configurations, the active orbitals are those of the $N = 3$, $2p_{3/2}$, $1f_{5/2}$, and $2p_{1/2}$ subshells and the $N = 4$, $1g_{9/2}$ intruder subshell. ^{66}Zn, being transitional nucleus, displays a complex spectrum and the description of its level structure from the viewpoint of a single model is difficult. Various theoretical approaches such as the spherical shell-model [35], crude shell model [17], deformed configuration mixing shell-model [36], Hartree-Fock-Bogoliubov calculation [37] and the two-proton cluster vibrator model [21,38] calculations have been used earlier to understand the positive parity and the negative parity level structures in ^{66}Zn.

Using the deformed configuration mixing shell model in the $p_{3/2}f_{5/2}p_{1/2}g_{9/2}$ model space, Ahalpara *et al.* have interpreted fairly well the positive parity high spin states in ^{66}Zn in terms of various configurations [36]. The observation of the sudden dip in the B(E2) value of the $8^+ \rightarrow 6^+$ transition has been attributed to the band crossing between

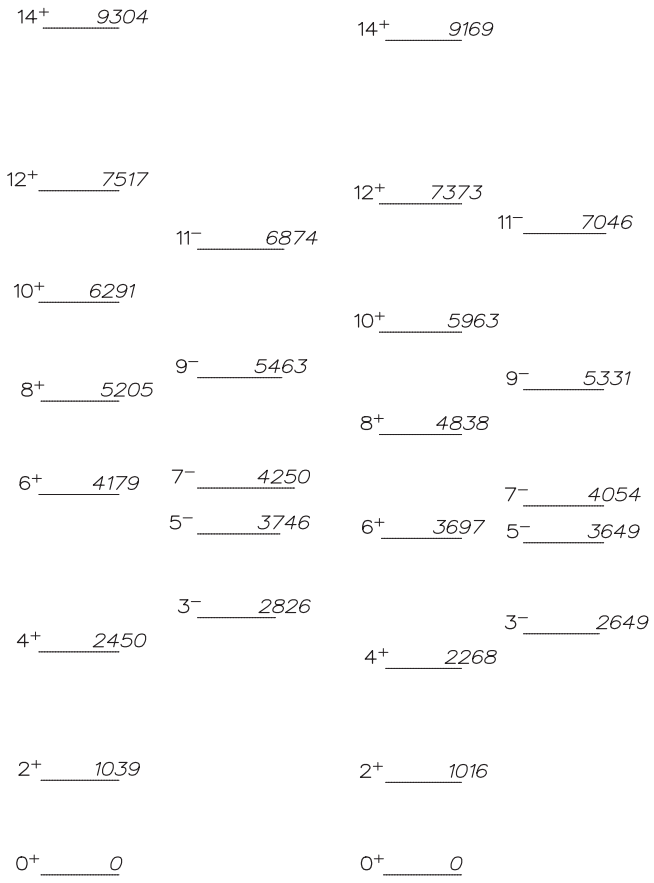

FIG. 3. Comparison of the yrast band and the negative parity level structure of ^{66}Zn (present work) and ^{68}Ge [9]. Numbers along the right side of the levels denote the level energies in keV and that in the left denote the spin(in $\hbar$)-parity.

the ground-state band and the deformed excited state band arising from the two particle-hole (2p-2h) excitation to the $1g_{9/2}$ orbital [36]. The ground-state band comprising of the $J^\pi = 0^+$, 2^+, 4^+, 6^+ states, has been assigned with the configuration $\pi\nu(p_{3/2}f_{5/2}p_{1/2})^{10}$ and the excited state band comprising of the 8^+, 10^+, 12^+, 14^+ states to the 2p-2h $(p_{3/2}f_{5/2}p_{1/2})^8(g_{9/2})^2$ configuration. Assuming a configuration of $[\pi(p_{3/2})^2\nu(f_{5/2}p_{1/2})^6]_{6^+} \otimes [\nu(g_{9/2})^2]_{8^+}$, a maximum spin of $14\hbar$ can be obtained and the corresponding (terminating) state has been observed in our work. Beyond this state, a change in the structure or shape transition can be expected which could be predicted by the theoretical calculations. Interestingly, in their calculations, Ahalpara *et al.* predicted the yrast 14^+ level (unobserved experimentally at that time) to lie at ≈9.4 MeV, which is very close to the experimentally observed 9.3 MeV level in the present work. In the present investigation, this band is also extended by the placement of the three new connecting γ-ray transitions of 1787, 519 and 1364 keV.

In terms of the level energy, intensity, and decay pattern, a great similarity of the level structure of ^{66}Zn with the neighboring ^{68}Ge isotope is observed. A comparison of the yrast and few negative parity level structure of ^{66}Zn with the isotonic ^{68}Ge is shown in Fig. 3. This kind of

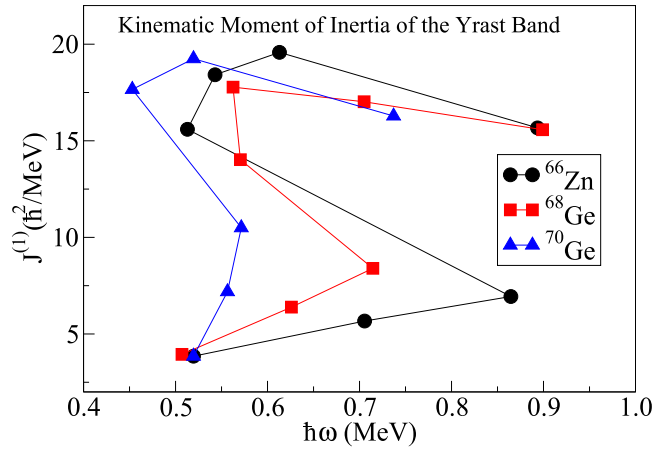

FIG. 4. Variation of the experimentally deduced kinematic moment of inertia as a function of the rotational frequency ($\hbar\omega$) for the yrast positive parity band in ^{66}Zn (present work). The corresponding values of the neighboring ^{68,70}Ge [9–11,14] isotopes are also shown for comparison.

comparison is useful in building the level structure systematics of nuclei in this mass region and in assigning the wave function configurations to the analogous quantum states. In ^{68,70}Ge, above the 6^+ state of the ground-state band, two 8^+ states appear leading to the forking of the ground-state band into two quadrupole excited bands [9–11,39]. Theoretical studies [40–42] have suggested this forking phenomena as the band-crossing of the ground-state band with the two excited deformed bands having the two-neutron $(\nu 1g^2_{9/2})$ and the two-proton $(\pi 1g^2_{9/2})$ quasiparticle configurations, respectively. Interestingly in ^{70}Ge, the simultaneous band crossing of the two-neutron aligned configuration and the γ band have been reported leading to the forking of the ground-state band [10].

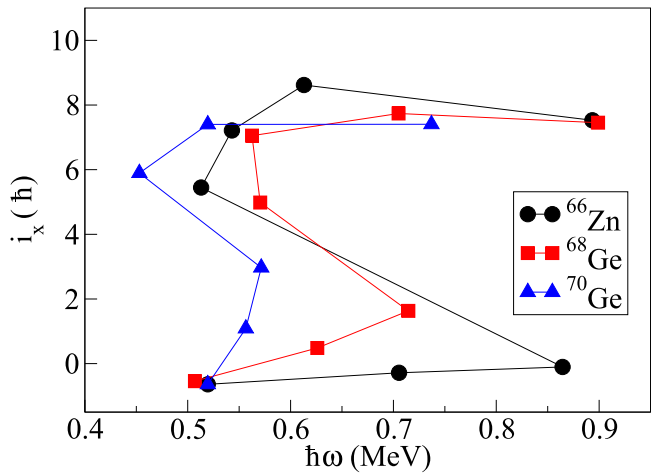

FIG. 5. Experimental alignments of the yrast positive parity band as a function of the rotational frequency for ^{66}Zn (present work) and ^{68,70}Ge [9–11]. The reference rotor, which was subtracted, is based on the Harris parameters, $J_0 = 6.0\hbar^2/\mathrm{MeV}$ and $J_1 = 3.5\hbar^4/\mathrm{MeV}^3$. Please see text for details.

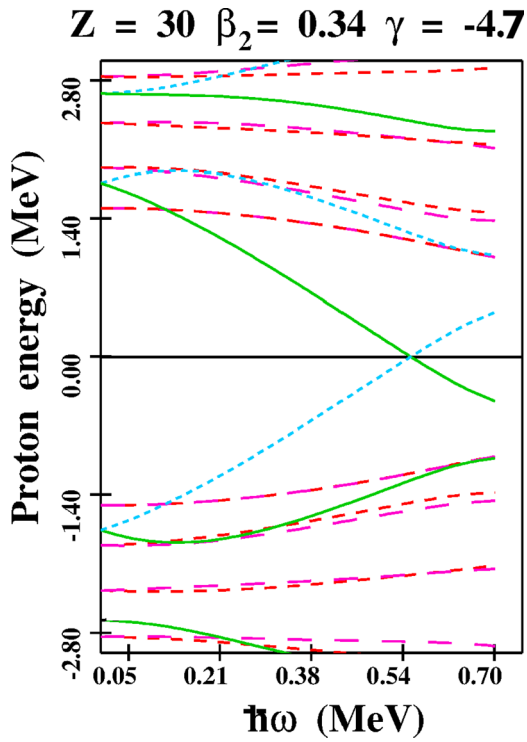

FIG. 6. Calculated quasiparticle Routhians for protons in ^{66}Zn as a function of the rotational frequency $\hbar\omega$ obtained from TRS calculation [44] for $\beta_2 = 0.34$ and $\gamma = -4.7^{\circ}$. Green and blue lines denote the positive parity, positive signature and positive parity, negative signature, respectively, whereas the red and magenta lines denote the negative parity, positive signature and the negative parity, negative signature respectively. Please see text for more details.

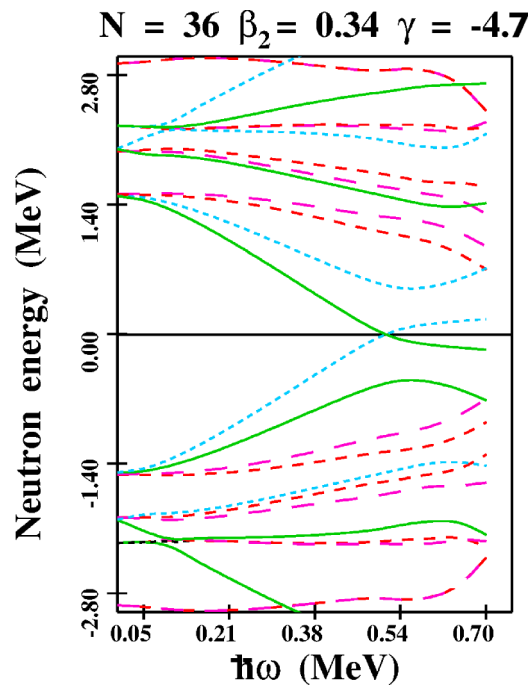

FIG. 7. Same as the Fig. 6 but for the neutrons. Please see text for details.

Figures 4 and 5 show the variation of the experimentally deduced kinematic moment of inertia and alignment, respectively, as a function of the rotational energy for ^{66}Zn for the observed yrast positive parity band consisting of 0^+, 2^+, 4^+, 6^+, 8^+, 10^+, 12^+, and 14^+ states. Here, the kinematic moment of inertia and the alignment are defined, respectively, as $J^{(1)} = i_x/\omega$ and $i = i_x - i_{\rm ref}$. It is to be noted here, that i_x is the x component (rotational component) of the total angular momentum and $i_{\rm ref}$ corresponds to the value of a reference rotor. The expressions for i_x and $i_{\rm ref}$ are, respectively,

$$i_x = \sqrt{I(I+1) - K^2}$$

and

$$i_{\rm ref} = (J_0 + \omega^2 J_1)\omega,$$

where K refers to the projection of the total angular momentum on the symmetry axis. J_0 and J_1 represent the Harris parameters. Here, the values of Harris parameters as accepted in this mass region are taken from the Refs. [10,11].

In both figures, the corresponding quantities for the nearby ^{68,70}Ge [9–11] isotopes are also shown for comparison. It is evident that the variation of the kinematic moment of inertia and the alignment as a function of the rotational frequency ($\hbar\omega$) in ^{66}Zn follow the same trend as that in ^{68,70}Ge, which in turn indicates a similar intrinsic structure of the observed bands in these three nuclei. The observed backbending in ^{68,70}Ge have been understood to be due to the alignment of a pair of neutrons in the $1g_{9/2}$ orbital [9,10]. As evident from the plots in the Figs. 4 and 5, the first alignment of a pair of neutrons in the $1g_{9/2}$ orbital in ^{68,70}Ge occurs at the frequencies of ≈ 0.60 MeV and ≈ 0.5 MeV, respectively.

The alignment plot for ^{66}Zn indicates that there is a total gain in the alignment of $\approx 8\hbar$ at a frequency of $\approx$0.6 MeV. To understand the observed alignment, quasiparticle Routhians for both the protons and neutrons have been calculated and are plotted, respectively, in the Figs. 6 and 7. The quasi-

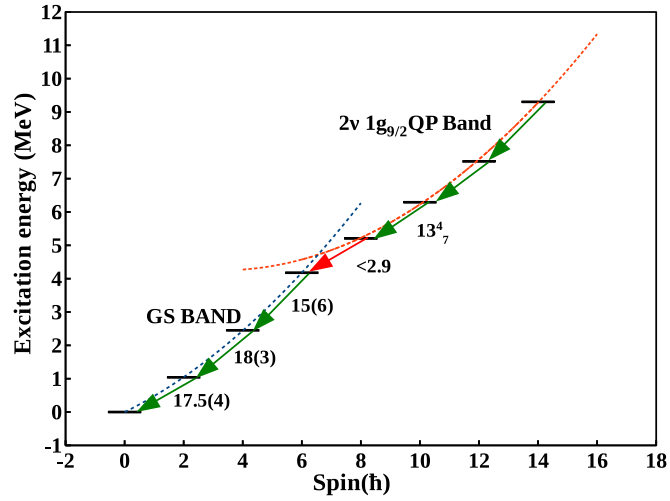

FIG. 8. Excitation energy vs. spin plot for the yrast bands of ^{66}Zn. Reduced transition probabilities B($E2$) of the corresponding γ-transitions, which are taken from the literature [43], are also plotted. The dashed lines represent the extrapolation of the bands through the second-order polynomial fitting.

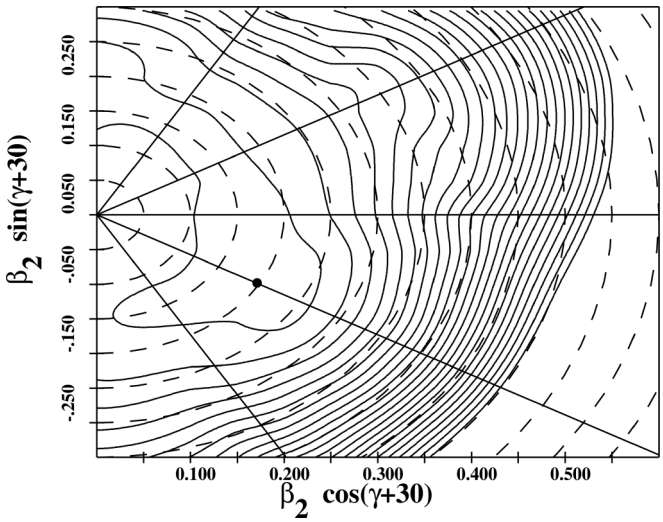

FIG. 9. Contour plots of the TRS calculations in ^{66}Zn for the zero quasiparticle (vacuum) at the rotational frequency($\hbar\omega$) 0.100 MeV. The energy separation between the two consecutive surface contours is 250 keV.

particle Routhians are calculated using TRS codes based on the Hartree-Fock-Bogoliuobov formalism [44], which is discussed later in this manuscript. These plots show that the first crossing of a neutron pair is possible at $\hbar\omega \approx 0.55$ MeV, while that for a pair of protons is feasible at $\hbar\omega > 0.70$ MeV. So, the band built on the 8^+ (5205 keV) state extending to the 14^+ can be understood to be due to the alignment of a pair of neutrons in the $1g_{9/2}$ orbital.

Band crossing has also been reported in the lighter ^{65}Zn isotope, where the two-proton alignment has been found to be responsible for the observed band crossing at a rotational frequency ~0.6 MeV [12] with the neutron alignment being blocked. The TRS calculations of ^{65}Zn have predicted that it undergoes a shape transition from a near oblate at lower spin to triaxial at intermediate spin [12]. In ^{66}Zn, the band

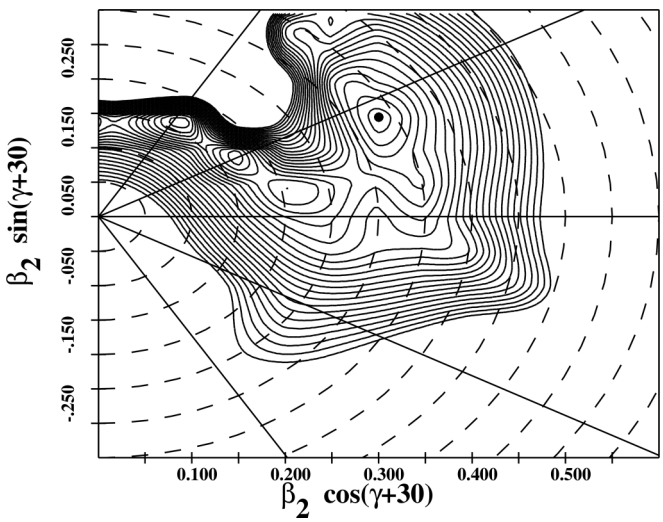

FIG. 10. Same as the Fig. 9 but for the 2-ν quasiparticle band (positive parity, positive signature) at $\hbar\omega = 0.5$ MeV in ^{66}Zn.

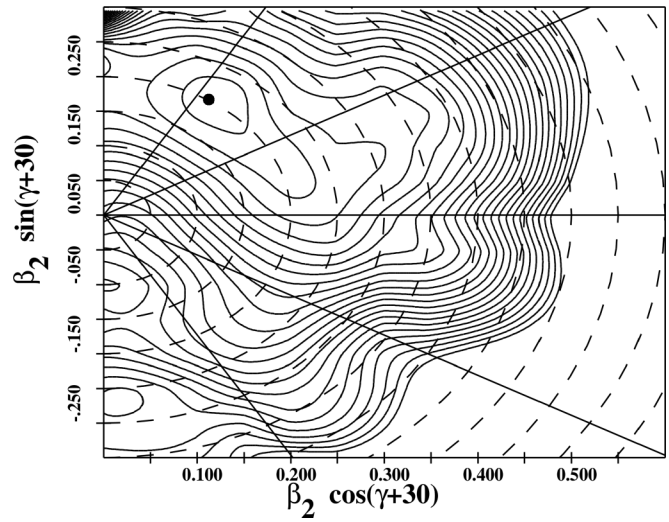

FIG. 11. Contour plots of the TRS calculations for the configuration $\pi(f_{5/2})^2 \otimes \nu(f_{5/2})^3(p_{3/2})^4(g_{9/2})^1$ of the negative parity quadrupole band like structure consisting of the 7^- (4250 keV), 9^- (5463 keV), and 11^- (6874 keV) states in ^{66}Zn at a rotational frequency($\hbar\omega$) 0.40 MeV. Here, the energy separation between the two consecutive surface contours is 250 keV.

crossing of the ground-state band and the two-quasiparticle band occurs at 6^+, which is evident from the sudden drop in the B(E2) value (<2.9 W.u.) for the $8^+ \rightarrow 6^+$, 1026 keV transition [43]. The band crossing is also apparent from the excitation energy vs spin plot for the yrast band illustrated in Fig. 8. The reduced transition probability [B(E2)] values for the transitions (J → J-2) de-exciting along the yrast line, which are taken from the literature [23,43] are also given in the plot. The bands are extrapolated by using a second order polynomial fitting and are given by dashed lines in the plot. The configuration of the two-quasiparticle band is certainly of a two-neutron character, i.e., $(\nu g_{9/2})^2$, as the proton alignment is known to occur at the higher frequencies and one can expect it to undergo a similar shape transition as ^{65}Zn [12] along the positive parity yrast band. However, the two-quasiproton aligned band could not be observed in this nucleus. This may be because of its light nature ($Z = 30, N = 36$), compared to the ^{68,70}Ge, leading to the unavailability of the $\pi 1g_{9/2}$ orbital near the proton Fermi surface. The two-neutron quasiparticle structure is well connected to the negative parity states (7^-, 9^-, 11^-), respectively, by the 955, 828, and the 643 keV transitions as seen from the level scheme. This may suggest the fact that these negative parity states also have the similar configurations as the positive parity band.

The TRS calculations for ^{66}Zn have been performed to understand the possible shape evolution using the Woods-Saxon potential. The Hartree-Fock-Bogoliuobov code of Nazarewicz *et al.* [44] has been used for the calculations. Equilibrium shapes were calculated in the β_2-γ plane with the minimization on the β_4 at different values of $\hbar\omega$. Shell corrections have been taken into account and as a residual interaction, the mono pole pairing force has been taken with the strength from Ref. [44]. Figures 9 and 10 show, respectively, the contour plots for the zero quasiparticle and the positive parity, positive

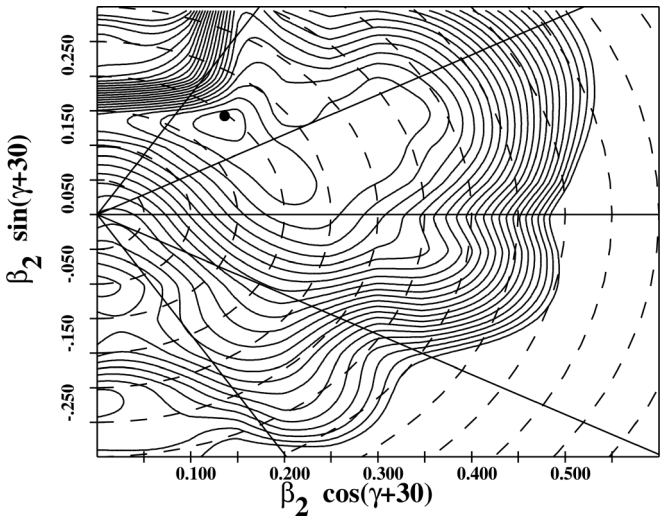

FIG. 12. Same as the Fig. 11 at the rotational frequency ($\hbar\omega$) 0.45 MeV.

signature two neutron quasiparticle sequence in ^{66}Zn. The calculation predicts a collective oblate shape of $\beta_2 \simeq 0.20$ at the lower frequencies up to $\hbar\omega = 0.25$ MeV albeit the flatness of the γ plane indicates a possible triaxial shape as shown in the Fig. 9. With the further increase of the rotational frequency the nucleus becomes more γ soft in nature, which means that the nucleus is triaxial in shape at intermediate spin. At a higher frequency of $\hbar\omega = 0.50$ MeV, it assumes a collective prolate shape having deformation $\beta_2 = 0.34$ ($\gamma \approxeq -4^\circ$) as evident from the plot in Fig. 10. These values of $\beta_2 = 0.34$ and $\gamma \approxeq -4^\circ$ have been used to calculate the quasiparticle Routhians (Figs. 6 and 7) from which the crossing frequencies are estimated. The TRS calculations thus predict that the alignment of a neutron pair drives the ^{66}Zn nucleus from a collective oblate shape at the ground state via the triaxial shape at the intermediate spin to a collective prolate shape at the high spin.

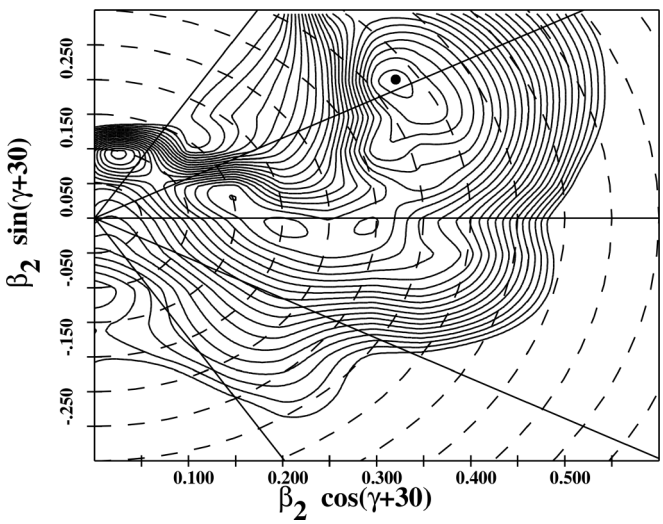

FIG. 13. Same as the Fig. 11 at the rotational frequency($\hbar\omega$) 0.55 MeV.

The configuration of the negative parity band consisting of the 7^- (4250 keV), 9^- (5463 keV), and 11^- (6874 keV) states is assumed to be of $\pi(f_{5/2})^2 \otimes \nu(f_{5/2})^3(p_{3/2})^4(g_{9/2})^1$. This configuration can generate a maximum angular momentum value of $13\hbar$ which is consistent with the observed highest spin state of the band. Figures 11, 12, and 13 represent the TRS plots for this configuration. As is evident from the plots, the TRS calculations for the negative parity band predict an evolution of shape from a moderately deformed ($\beta_2 \approx 0.20$, $\gamma \approx 23^\circ$) triaxial at $\hbar\omega = 0.40$ MeV to well deformed ($\beta_2 \approx 0.37$, $\gamma \approx 3^\circ$) prolate at $\hbar\omega = 0.55$ MeV.

V. CONCLUSION

Excited states of ^{66}Zn have been studied following their population in a heavy-ion induced fusion-evaporation reaction and using an array of the 14 Compton suppressed clover detectors. Combining the measurement of the energy, angular correlation, linear polarization, intensity and coincidence relationship of the emitted γ-rays, the level scheme of ^{66}Zn has been constructed. With 14 new transitions being identified, the level scheme of this nucleus has been extended up to the excitation energy ≈12.3 MeV and a tentative spin of $(17^+)\hbar$. Further, the positive parity $[\pi(p_{3/2})^2\nu(f_{5/2}p_{1/2})^6] \otimes [\nu(g_{9/2})^2]$ yrast band and the negative parity band corresponding to the $\pi(f_{5/2})^2 \otimes \nu(f_{5/2})^3(p_{3/2})^4(g_{9/2})^1$ configuration have been identified up to their terminating states. A qualitative discussion of the observed band crossing phenomenon and the structure of other levels were presented in the light of various quasiparticle configurations which are based on the existing theoretical studies for this nucleus and the other neighboring nuclei (viz. ^{68,70}Ge). TRS calculations predict a shape transition of this nucleus from a collective oblate at $\hbar\omega = 0.10$ MeV to a collective prolate at $\hbar\omega = 0.55$ MeV via triaxial shapes at the intermediate spins along the positive parity yrast band. This shape transition has been attributed to the alignment of a pair of neutron in the $1g_{9/2}$ orbital. Similar TRS calculations corresponding to the negative parity quadrupole band predict an evolution of the shape from the triaxial with a moderate deformation to the prolate with a higher deformation value. Thus, the present study points towards the established fact that the unique parity $1g_{9/2}$ orbital unequivocally plays a major role in the underlying structure of this nucleus as is observed in this work.

ACKNOWLEDGMENTS

The authors thank the operating crew of the Pelletron facility and the target laboratory at IUAC, New Delhi for providing excellent support throughout the experiment. We thank S. Nandi (VECC, Kolkata), S.S. Bhattacharjee (IUAC), and R. Garg (IUAC) for their help during the experiment. Constant encouragement from D. Kanjilal (IUAC) is gratefully acknowledged. We acknowledge the financial assistance received from the IUAC (New Delhi) via Project No. UFR-49318, SERB-DST (India) via Project No. EMR/2015/000891, and DAE-BRNS (India), Project No. 37(3)/14/17/2016-BRNS.

[1] D. Rudolph *et al.*, Phys. Rev. L **80**, 3018 (1998).
[2] C. E. Svensson *et al.*, Phys. Rev. L **82**, 3400 (1999).
[3] A. Galindo-Uribarria *et al.*, Phys. Lett. B **422**, 45 (1998).
[4] D. Karlgren *et al.*, Phys. Rev. C **69**, 034330 (2004).
[5] J. Gellanki *et al.*, Phys. Rev. C **86**, 034304 (2012).
[6] M. Albers *et al.*, Phys. Rev. C **94**, 034301 (2016).
[7] M. Devlin *et al.*, Phys. Rev. L **82**, 5217 (1999).
[8] U. S. Ghosh *et al.*, Phys. Rev. C **102**, 024328 (2020).
[9] D. Ward *et al.*, Phys. Rev. C **63**, 014301 (2000).
[10] M. Kumar Raju *et al.*, Phys. Rev. C **93**, 034317 (2016).
[11] B. Mukherjee *et al.*, Act. Phys. Hung.: HIP **13**, 253 (2001).
[12] B. Mukherjee, S. Muralithar, R. P. Singh, R. Kumar, K. Rani, R. K. Bhowmik, S. C. Pancholi, Phys. Rev. C **64**, 024304 (2001).
[13] E. A. Stefanova *et al.*, Phys. Rev. C **67**, 054319 (2003).
[14] R. A. Haring-Kaye, S. I. Morrow, J. Döring, S. L. Tabor, K. Q. Le, P. R. P. Allegro, P. C. Bender, R. M. Elder, N. H. Medina, J. R. B. Oliveira, and V. Tripathi, Phys. Rev. C **97**, 024308 (2018).
[15] A. Gade, H. Klein, N. Pietralla, P. von Brentano, Phys. Rev. C **65**, 054311 (2002).
[16] P. M. Endt *et al.*, Nucl. Phys. A **575**, 297 (1994).
[17] A. Boucenna, L. Kraus, I. Linck, T. U. Chan, Phys. Rev. C **42**, 1297 (1990).
[18] G. P. Couchell *et al.*, Phys. Rev. **161**, 1147 (1967).
[19] J. F. Braundet *et al.*, Phys. Rev. C **12**, 1739 (1975).
[20] G. F. Neal *et al.*, Nucl. Phys. A **280**, 161 (1977).
[21] L. Cleemann *et al.*, Nucl. Phys. A **386**, 367 (1982).
[22] B. Erlandsson *et al.*, Phys. Scr. **22**, 432 (1980).
[23] C. Morand *et al.*, J. Phys. Fr. **38**, 1319 (1977).
[24] D. Kanjilal *et al.*, Nucl. Instrum. Methods Phys. Res. Sect., A **328**, 97 (1993).
[25] S. Muralithar *et al.*, Nucl. Instrum. Methods Phys. Res. Sect., A **622**, 281 (2010).
[26] B. P. Ajith Kumar *et al.*, in *Proceedings of the 44th DAE-BRNS Symposium on Nuclear Physics* (Department of Atomic Energy, Government of India, Mumbai, 2001), p. 390.
[27] R. K. Bhowmik *et al.*, in *Proceedings of the 44th DAE-BRNS Symposium on Nuclear Physics* (Department of Atomic Energy, Government of India, Mumbai, 2001), p. 422.
[28] D. C. Radford, Nucl. Instrum. Methods Phys. Res., Sect. A **361**, 290 (1995).
[29] K. S. Krane *et al.*, Nucl. Data Tables **11**, 351 (1973).
[30] K. Starosta *et al.*, Nucl. Instrum. Methods Phys. Res., Sect. A **423**, 16 (1999).
[31] R. Palit *et al.*, Pramana J. Phys. **54**, 347 (2000).
[32] S. Rai *et al.*, Eur. Phys. J. A **54**, 84 (2018).
[33] U. S. Ghosh *et al.*, Phys. Rev. C **100**, 034314 (2019).
[34] S. Rai, Ph.D. thesis, Visva-Bharati University (2019).
[35] J. F. A. Van Heinen *et al.*, Nucl. Phys. A **269**, 159 (1976).
[36] D. P. Ahalpara *et al.*, Nucl. Phys. A **371**, 210 (1981).
[37] S. K. Sharma, Phys. Rev. C **22**, 2612 (1990).
[38] V. Lopac and V. Paar, Nucl. Phys. A **297**, 471 (1978).
[39] U. Hermkens *et al.*, Z. Phys. A **343**, 371 (1992).
[40] A. P. de Lima *et al.*, Phys. Rev. C **23**, 213 (1981).
[41] P. A. Dar, R. Devi, S. K. Khosa, J. A. Sheikh, Phys. Rev. C **75**, 054315 (2007).
[42] M. Hasegawa, K. Kaneko, T. Mizusaki, Phys. Rev. C **70**, 031301(R) (2004).
[43] ENSDF Database, https://www.nndc.bnl.gov/ensdf.
[44] W. Nazarewicz *et al.*, Nucl. Phys. A **512**, 61 (1990).